



Chemical compositions and source identification of PM_{2.5} aerosols for estimation of a diesel source surrogate

Manoranjan Sahu^a, Shaohua Hu^a, Patrick H. Ryan^b, Grace Le Masters^b, Sergey A. Grinshpun^b, Judith C. Chow^c, Pratim Biswas^{a,*}

^a Aerosol and Air Quality Research Laboratory, Department of Energy, Environmental and Chemical Engineering, Washington University in St. Louis, St. Louis, MO, USA

^b Department of Environmental Health, University of Cincinnati, Cincinnati, OH, USA

^c Division of Atmospheric Sciences, Desert Research Institute, Reno, NV, USA

ARTICLE INFO

Article history:

Received 10 July 2010

Received in revised form 8 March 2011

Accepted 24 March 2011

Available online 14 April 2011

Keywords:

PM_{2.5}

Receptor modeling

Diesel exhaust

Gasoline exhaust

Elemental carbon

Organic carbon

ABSTRACT

Exposure to traffic-related pollution during childhood has been associated with asthma exacerbation, and asthma incidence. The objective of the Cincinnati Childhood Allergy and Air Pollution Study (CCAAPS) is to determine if the development of allergic and respiratory disease is associated with exposure to diesel engine exhaust particles. A detailed receptor model analyses was undertaken by applying positive matrix factorization (PMF) and UNMIX receptor models to two PM_{2.5} data sets: one consisting of two carbon fractions and the other of eight temperature-resolved carbon fractions. Based on the source profiles resolved from the analyses, markers of traffic-related air pollution were estimated: the elemental carbon attributed to traffic (ECAT) and elemental carbon attributed to diesel vehicle emission (ECAD).

Application of UNMIX to the two data sets generated four source factors: combustion related sulfate, traffic, metal processing and soil/crustal. The PMF application generated six source factors derived from analyzing two carbon fractions and seven factors from temperature-resolved eight carbon fractions. The source factors (with source contribution estimates by mass concentrations in parentheses) are: combustion sulfate (46.8%), vegetative burning (15.8%), secondary sulfate (12.9%), diesel vehicle emission (10.9%), metal processing (7.5%), gasoline vehicle emission (5.6%) and soil/crustal (0.7%). Diesel and gasoline vehicle emission sources were separated using eight temperature-resolved organic and elemental carbon fractions. Application of PMF to both datasets also differentiated the sulfate rich source from the vegetative burning source, which are combined in a single factor by UNMIX modeling. Calculated ECAT and ECAD values at different locations indicated that traffic source impacts depend on factors such as traffic volumes, meteorological parameters, and the mode of vehicle operation apart from the proximity of the sites to highways. The difference in ECAT and ECAD, however, was less than one standard deviation. Thus, a cost benefit consideration should be used when deciding on the benefits of an eight or two carbon approach.

Published by Elsevier B.V.

1. Introduction

Exposure to traffic-related particles during childhood has been shown to exacerbate existing asthma including decreased lung function (Trenga et al., 2006), emergency department visits (Sun et al., 2005), wheezing in early infancy and childhood (Ryan et al., 2007, 2009) and medication use (Schildcrout et al., 2006). Recently, Jerrett et al. (2008) demonstrated an association between exposure

to traffic-related pollution and the development of asthma. Traffic-related sources represented by vehicular exhaust, contribute a major fraction to total ambient PM (Chow et al., 2007; Shi et al., 1999; Watson et al., 2008) and are comprised of metals, organic polycyclic aromatic hydrocarbons (PAH), secondary sulfate and nitrate, and elemental and organic carbon (EC and OC, respectively) (Hetland et al., 2005; Wichmann, 2007). Particles arising from traffic sources are of particular interest because of size (primarily fine, PM_{2.5} and ultrafine, PM_{0.1}), chemical composition, and shape (morphology). The characteristics of traffic-originated particles enable them to penetrate the upper and lower airways and translocate to other tissues including the brain (Kreyling et al., 2002). Approximately 92% of diesel engine exhaust particulates (DEP) by mass concentration are within the ultrafine size range resulting in high particle density concentrations that reach and deposit in the nasal and peripheral

* Corresponding author at: Aerosol and Air Quality Research Laboratory, Department of Energy, Environmental and Chemical Engineering, Campus Box 1180, Washington University in St. Louis, St. Louis, MO, 63130, USA. Tel.: +1 314 935 5548; fax: +1 314 935 5464.

E-mail address: pratim.biswas@wustl.edu (P. Biswas).

airways upon inhalation (EPA, 2002). Inhalation of DEP generates reactive oxygen species (ROS), inducing oxidative stress on nasal mucosal and bronchial epithelial cells leading to increased mucus production, disruption of the respiratory epithelial barrier and increased airway hyper responsiveness (Riedl and Diaz-Sanchez, 2005). DEP also possess immune adjuvant properties capable of enhancing local nasal production of allergic cytokines and specific IgE responses (e.g., IL-4) to inhaled aeroallergens, particularly in the nasal airway (Pandya et al., 2002). Recently, studies have suggested that particles arising from gasoline combustion may demonstrate similar toxicity to DEP (Seagrave et al., 2002).

The objective of the Cincinnati Childhood Allergy and Air Pollution Study (CCAAPS), a longitudinal birth cohort study, is to determine if exposure to DEP during infancy and early childhood is associated with the development of allergic disease and asthma (Martuzevicius et al., 2004). In order to examine the relationship between exposure to traffic-related air pollutants and health effects in the CCAAPS cohort, a land-use regression (LUR) model was developed. This LUR model utilized a marker of traffic-related particles thought to be dominated by DEP (Ryan et al., 2007, 2008), the fraction of elemental carbon attributable to traffic (ECAT). ECAT was derived by applying two commonly used receptor modeling techniques for source apportionment to ambient data, positive matrix factorization (PMF) and UNMIX (Henry, 2003; Kim and Hopke, 2004a; Lee et al., 2006; Lewis et al., 2003; Maykut et al., 2003; Polissar et al., 2001). Hu et al. (2006) applied UNMIX receptor modeling to $PM_{2.5}$ data collected at two CCAAPS sampling sites in order to identify four possible major polluting sources: 1) combustion related sulfate sources, 2) traffic-related sources, 3) metal processing industries and 4) soil/crustal sources. In the CCAAPS cohort, exposure to increased levels of ECAT during infancy was associated with wheezing prior to age one (Ryan et al., 2007). Further, children exposed to high levels of ECAT and endotoxin in their home prior to age one had greater than a five-fold increased risk for persistent wheezing at age three when compared to children exposed to low levels of ECAT and endotoxin (Ryan et al., 2009). Sucharew et al. (2010) reported that traffic exhaust exposure (quantified by ECAT) may be a risk factor for night cough in young children.

More recently, source sampling of diesel and gasoline vehicular emissions and subsequent analysis of the carbon fractions by the temperature resolved thermal optical method indicates that gasoline and diesel sources can be differentiated based on the abundance of individual carbon sub fractions (Cao et al., 2006; Chow et al., 2004; Watson et al., 1994). OC and EC fractions and the organic pyrolyzed organic carbon (OPTRC) are measured at different temperature steps. PMF receptor modeling analysis using temperature resolved eight carbon fractions for $PM_{2.5}$ data from Seattle, WA (Maykut et al., 2003), Atlanta, GA (Kim et al., 2004), Washington, DC (Kim and Hopke, 2004b), Georgia and Alabama (Liu et al., 2006), and St. Louis (Lee et al., 2006) illustrated that diesel and gasoline vehicle sources can be delineated.

The objective of this study was to improve the identification of source contributions by differentiating gasoline and diesel vehicle emissions using temperature resolved eight carbon fractions. In addition, the potential for combining the sampling data obtained at different sites into one dataset for source apportionment when the sampling sites are in close proximity was examined. UNMIX and PMF are applied to the same dataset containing only EC and OC carbon fractions estimated by the NIOSH method. In addition, UNMIX and PMF are applied to eight temperature resolved carbon fractions estimated by the IMPROVE protocol (Chow et al., 1993). The major sources identified by both modeling techniques are compared. The EC attributed to individual traffic sources (diesel and gasoline) is derived based on the resolved sources from the receptor modeling.

2. Materials and methods

2.1. Ambient $PM_{2.5}$ sampling and chemical analysis methods

For the epidemiological study undertaken in the Greater Cincinnati area, sampling was conducted at 24 sites of the CCAAPS network (Fig. 1). Details regarding the monitoring sites can be found in previous publications (Hu, 2007; Hu et al., 2006). Ambient data obtained at eleven selected sites between 2002 and 2006 were utilized for this analysis. These extensive data base provides more representative source profiles and contributions than modeling conducted with a few datasets.

Twenty-four hour integrated ambient air sampling was conducted nominally from 0900 am to 0900 pm (+1 day). 37-mm Teflon-membrane filters (nominal pore size = 1 μ m) (Pall Corporation) and 37-mm quartz-filters (Whatman Inc) with Harvard-type impactors (Air Diagnostics and Engineering Inc.) were used for collecting $PM_{2.5}$ samples. Teflon filters were conditioned at a temperature of 22–24 °C with a humidity of 30–40% for at least 24 h for temperature and humidity equilibration at Washington University in St. Louis (Hu et al., 2006). The difference in weight of the filter samples after sampling and before sampling were used to determine the $PM_{2.5}$ mass concentrations. X-ray fluorescence (XRF) technique was used to analyze the Teflon filters for ambient elemental concentrations (Chester Labnet). A total of 39 elements were analyzed and 15 chemical species (Al, Si, S, K, Ca, Ti, Cr, Mn, Fe, Ni, Cu, Zn, Se, Br, and Pb) were consistently present in the analyzed samples (Hu et al., 2006). More details regarding the advantage of XRF elemental measurements, quality control, and comparison with other methods can be found in our previous studies (Reponen et al., 2003; Martuzevicius et al., 2004). The detailed sampling procedure and analytical methods adopted for the CCAAPS network sampling sites are described elsewhere (Hu, 2007; Martuzevicius et al., 2004).

The quartz filters were sectioned into two halves to measure the carbon fractions. The first half of the filters was analyzed by the thermal optical transmittance (TOT) technique using the NIOSH-5040 method (Birch and Cary, 1996) to determine EC and OC concentrations (Sunset Lab). The other half was frozen, preserved, and then analyzed by the Interagency Monitoring of Protected Visual Environments (IMPROVE) thermal optical reflectance (TOR) protocol (Chow et al., 1993) for eight temperature resolved carbon fractions (Desert Research Institute). According to this protocol, OC fractions are measured at four different temperature steps: O1TC at 120 °C, O2TC at 250 °C, O3TC at 450 °C, and O4TC at 550 °C in 100% helium (He) atmosphere. The three EC fractions were measured in a mixture of 2% oxygen/98% He: E1TC at 550 °C, E2TC at 700 °C, and E3TC at 800 °C. Pyrolyzed carbon (OPTRC) was determined based on the laser response (laser reflectance is monitored until it returned to its initial value). In IMPROVE method, EC1 measurement includes OPTRC. In this study, OPTRC has been subtracted from the EC1 before using as an independent variable in the modeling. The detailed analysis procedure for the eight carbon fractions has been described in Chow et al. (1993, 2007). The total carbon was estimated by this method as $TC = OC (O1TC + O2TC + O3TC + O4TC + OPTRC) + EC (E1TC + E2TC + E3TC)$. In this study, 203 samples were used for which both the EC and OC concentration measurements and eight carbon fraction measurements were available. To directly compare the source estimates from the model, sampling data sets with samples having both carbon fractions and temperature resolved eight carbon fraction measurements were used.

Data from all the sampling stations were combined to form large datasets, which is a step forward from the earlier receptor modeling study that relied on a few samples collected at the CCAAPS sampling sites (Hu et al., 2006). The CCAAPS sampling sites are very closely located within a dimension of 35 km \times 40 km. The pollutants from any local source will have a fair chance to have potential impact on

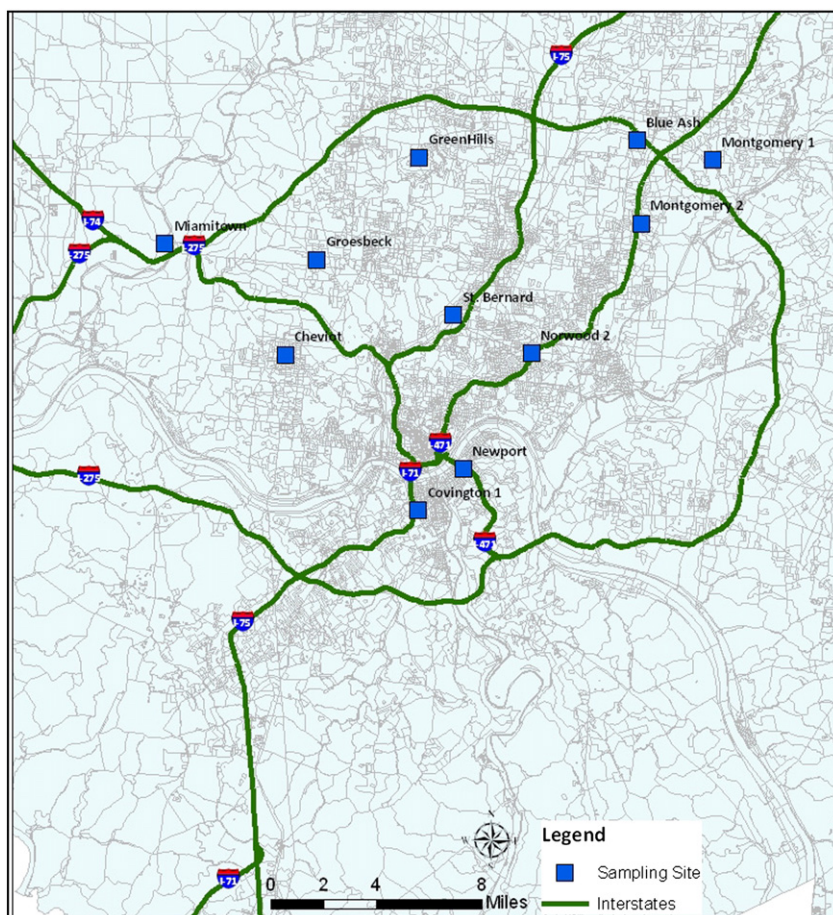


Fig. 1. Schematic diagram of the sampling locations (24 Cincinnati Childhood Allergy and Air Pollution Study (CCAAPS) sampling sites). Abbreviation of the sampling locations is given below. Blue Ash (BLU), Brighton (BRI), Cheviot (CHE), Covington1 (COV1), Green Hills (GRE), Groesbeck (GRO), Montgomery1 (MON1), Montgomery 2 (MON2), Newport (NEW), Norwood2 (NOR2), and St. Bernard (STB).

receptors anywhere within the CCAAPS sampling network, during the 24-h sampling period. The relative strength of the impact on an individual receptor is dependent on the proximity of that receptor to the source, but the source profiles will be the same for different receptors. However, combining the data from all the sites into one dataset may produce higher uncertainties in model predictions.

3. Model description and calculation

Receptor modeling assumes mass conservation to apportion different source categories for ambient particulate matter. It can be explained in general terms as the impact of N independent sources on the receptor site for all chemical species in a given sample:

$$x_{ij} = \sum_{k=1}^N g_{ik} f_{kj} + \varepsilon_{ij} \quad (1)$$

where x_{ij} is the j th species concentration measured in the i th sample, g_{ik} is the particulate mass concentration from the k th source contributing to the i th sample. f_{kj} is the j th species mass fraction in the k th source and ε_{ij} is the error estimate.

UNMIX (Henry, 2003) and PMF (Maykut et al., 2003; Paatero, 1997; Polissar et al., 2001) provide solution to Eq. (1) based on two different mathematical approaches. UNMIX determines the edges in the dataset. The number and direction of the edges depend on the number of species chosen for the UNMIX model. UNMIX incorporates the algorithm "NUMFACT" that estimates the number of factors in the data using principal component analysis on randomly sampled subsets of the original data (Henry, 2003). PMF derives a solution

that minimizes an object function, Q , which is determined based on the uncertainties associated with individual measured data, subject to nonnegative constraints (Polissar et al., 2001). The objective function is defined as:

$$Q = \sum_i^n \sum_{k=1}^m \left[\frac{x_{ik} - \sum_{k=1}^N g_{ik} \times f_{kj}}{\sigma_{ij}} \right]^2 \quad (2)$$

where σ_{ij} is an uncertainty estimate in the j th species measured in the i th sample. A PMF solution is not as sensitive as UNMIX to the choice of input species. The combined dataset has been analyzed by both UNMIX (EPA UNMIX 6.0) and PMF (EPA PMF 3.0) to identify the source profiles and contributions. Details about both UNMIX and PMF modeling techniques can be found in the literature (Henry, 2003; Paatero, 1997).

Some of the key aspects of the receptor modeling approach are post processing of the datasets, identifying the outliers in the datasets, and assigning uncertainty to the measured species, all of which influence the modeling results. For UNMIX modeling, species having a signal/noise ratio greater than 2 and a minimum R^2 of 0.8 were used to filter the sources. For initial runs, good edge species obtained by plotting the $PM_{2.5}$ mass versus species concentration were chosen to find minimum possible solution (Henry, 2003; Hu et al., 2006). Additional species were included to test the stability of the solution and determine if this measure could enhance the identification of sources with respect to the number and resolution. For datasets

consisting of two carbon fractions, species chosen for the model runs were, EC, OC, Al, Si, S, Fe, Cu, Zn, Ca, Se, Pb, Ti, and Ca. For datasets consisting of eight carbon fractions species chosen were O1TC, O2TC, O3TC, O4TC, OPTRC and E1TC in place of EC and OC fractions. However, with the addition of the E2TC and E3TC fractions, feasible solutions for source profiles could not be found. For the chosen four source factor solutions, the minimum $R^2 = 0.82$ and signal/noise ratio was 3.31 for the eight temperature resolved carbon fractions, and $R^2 = 0.84$ and signal/noise ratio equal to 2.73 for the two non-temperature resolved carbon fractions. When more species were added, five sources were resolved. Since many species concentrations were negative in one of the resolved profiles, a four-source solution was finally chosen for this study.

In PMF modeling, the number of factors is determined by experimenting and finding the optimal number based on the physical meaningful sources. The uncertainty values for the different species were chosen according to the values reported for the U.S EPA Speciation Trends Network (STN; part of the Chemical Speciation Network [CSN]) (Kim et al., 2005). To minimize the influence of extreme values on the PMF solution, a robust mode was chosen in this study. Based on the signal/noise ratio of the species, values less than 1.5 were qualified as weak. For some of the species, O1TC, OPTRC and E1TC were assigned higher uncertainty because of the uncertainty associated with their measurements (Kim and Hopke, 2004b; Kim et al., 2004). The resulting PMF source profiles were derived based on trial and error evaluation of the solutions.

4. Results and discussion

4.1. Ambient $PM_{2.5}$ concentration

The $PM_{2.5}$ and elemental concentrations differed between sampling sites. The locations near interstate highways, the main pathway for heavy diesel vehicles, showed higher levels of EC and traffic-related elements such as Fe, Cu, Mn, Pb, Al and Si.

The average $PM_{2.5}$ concentration ranged from $12.6 \pm 5.1 \mu\text{g}/\text{m}^3$ at Groesbeck to $24.2 \pm 19.5 \mu\text{g}/\text{m}^3$ at Newport. The major reason for variation is the site location. The Newport site is located in the downtown area which is very close to I-471 while the Groesbeck site is in suburban area within 400 m from the Ronald Reagan highway. The average $PM_{2.5}$ concentrations as well as the concentrations of metals are presented in Table 1 for all the sampling locations. Overall, a lower spatial variation in $PM_{2.5}$ (CV = 21%) was observed throughout the sampling periods. Martuzevicius et al. (2004) measured the spatial and temporal variation of the $PM_{2.5}$ concentration and composition at 11 locations of CCAAPS during the field campaign from December 2001 to November 2002 and found very little variation in $PM_{2.5}$, which is consistent with the observations of this study. However, the temporal variations in $PM_{2.5}$ concentration observed at specific sites in this study were relatively high with the coefficient of variation ranging from 26% to 80%. The low overall variation in $PM_{2.5}$ concentration may be due to high temporal variation in $PM_{2.5}$, and indicates the contribution of regional sources and long range atmospheric transport of the fine particulate matter (Gehrig and Buchmann, 2003; Martuzevicius et al., 2004). The concentration was greater at city centers than in suburban and rural areas, which likely resulted from the merger of interstate highways and increased traffic near the city.

4.2. Elemental composition of ambient $PM_{2.5}$

As many as 39 elements were analyzed by XRF. Table 1 summarizes the results obtained after blank were subtracted for the elements, which were present in significant amounts and/or served as markers for relevant sources. Among crustal element concentrations, the average aluminum varied from 14.1 ± 13.2 to $84.3 \pm 67.5 \text{ ng}/$

Table 1
Average $PM_{2.5}$ concentrations and its elemental compositions of samples collected at different sites.

Sampling site	$PM_{2.5}$ concentration ($\mu\text{g}/\text{m}^3$)	Elemental composition of $PM_{2.5}$ (ng/m^3)										Other metals
		EC ($\mu\text{g}/\text{m}^3$)	OC ($\mu\text{g}/\text{m}^3$)	Na	Al	K	Ca	Si	Fe	Zn	S	
Brighton (29)	17.7 ± 8.5	1.2 ± 0.7	3.5 ± 1.9	54.6 ± 51.2	60.1 ± 121.9	69.1 ± 36.5	138.5 ± 86.3	168.2 ± 242.2	181.1 ± 124.9	65.9 ± 111.1	1358.10 ± 895.9	70.9 ± 44.1
Cheviot (35)	18.4 ± 9.8	0.5 ± 0.3	3.3 ± 1.6	39.8 ± 35.8	48.7 ± 87.0	69.2 ± 58.2	64.3 ± 35.8	118.9 ± 174.9	89.7 ± 59.1	14.3 ± 8.2	2035.8 ± 1456.9	44.6 ± 21.2
Montgomery 1 (20)	16.4 ± 10.7	0.4 ± 0.2	3.3 ± 1.6	33.6 ± 42.1	30.1 ± 25.9	67.8 ± 42.8	46.7 ± 22.9	65.9 ± 42.3	70.2 ± 34.7	15.9 ± 14.6	1515.3 ± 1121.1	38.9 ± 22.1
Covington 1 (21)	23.2 ± 10.5	0.9 ± 0.5	4.8 ± 1.4	78.5 ± 102.2	31.1 ± 18.1	60.7 ± 24.7	78.7 ± 36.0	91.1 ± 40.2	133.5 ± 79.0	12.8 ± 5.7	2257.6 ± 1389.3	50.7 ± 20.3
Norwood 2 (33)	19.8 ± 9.4	0.8 ± 0.5	4.0 ± 1.6	46.4 ± 49.2	48.4 ± 27.6	71.5 ± 31.4	88.8 ± 54.8	118.9 ± 71.7	148.0 ± 85.3	33.0 ± 21.1	1589.1 ± 1054.7	57.1 ± 20.9
Montgomery 2 (12)	13.2 ± 5.2	0.4 ± 0.2	2.5 ± 1.3	40.1 ± 29.3	26.2 ± 23.1	52.0 ± 9.8	52.5 ± 25.8	60.9 ± 33.8	73.0 ± 50.6	12.6 ± 7.9	1301.0 ± 740.4	32.8 ± 7.7
Newport (9)	24.2 ± 19.5	0.5 ± 0.2	3.0 ± 0.6	139.2 ± 241.8	30.0 ± 13.2	73.9 ± 29.5	115.5 ± 61.8	105.2 ± 42.4	140.1 ± 57.0	18.6 ± 9.8	1369.4 ± 760.8	87.8 ± 132.9
Blue Ash (10)	14.2 ± 3.9	0.3 ± 0.1	1.6 ± 0.8	27.3 ± 241.8	14.1 ± 13.2	44.0 ± 29.5	32.9 ± 61.8	34.2 ± 42.4	56.6 ± 57.0	30.7 ± 9.8	1204.4 ± 760.8	28.9 ± 132.9
Green Hills (15)	15.8 ± 8.1	0.3 ± 0.2	2.3 ± 1.3	38.1 ± 40.1	30.6 ± 23.1	55.4 ± 23.0	43.8 ± 27.4	69.9 ± 46.8	59.1 ± 27.8	13.2 ± 7.1	1647.0 ± 1177.5	29.9 ± 14.2
St. Bernard (10)	15.4 ± 7.3	1.3 ± 0.8	4.1 ± 2.8	71.4 ± 65.3	84.4 ± 67.5	84.9 ± 61.2	306.1 ± 358.6	290.7 ± 265.2	302.9 ± 316.5	37.0 ± 25.4	946.3 ± 294.4	97.8 ± 81.4
Groesbeck (9)	12.6 ± 5.1	0.4 ± 0.1	2.6 ± 1.0	37.5 ± 21.8	24.2 ± 10.7	52.5 ± 19.1	58.5 ± 18.9	78.1 ± 32.1	65.7 ± 34.4	13.5 ± 9.6	1079.5 ± 792.8	32.6 ± 8.5

m^3 , silicon from 34.2 ± 42.4 to 290.7 ± 265.2 ng/m^3 , and calcium from 32.9 ± 61.8 to 306.1 ± 358.6 ng/m^3 ; all with the lowest levels at Blue Ash and the highest at St. Bernard.

Among traffic source elemental concentrations, iron varied from 56.6 ± 57.0 ng/m^3 (Blue Ash) to 302.9 ± 316.5 ng/m^3 (St. Bernard), and zinc varied from 12.6 ± 7.9 ng/m^3 (Montgomery2) to 65.9 ± 111.0 ng/m^3 (Bridgeton). The relative abundance of different trace elements varied depending on the locations and relative impact of the local pollution sources. Calcium, silicon and iron concentrations were relatively higher at Brighton, St. Bernard and Newport compared to other locations. The relatively higher variation in the trace elements compared to $PM_{2.5}$ indicates that these elements originated mostly from local pollution sources. The concentration of sulfur ranged from 946.3 ± 294.4 ng/m^3 (St. Bernard) to 2257.6 ± 1389.3 ng/m^3 (Covington1). Sulfur showed the highest concentration among all the elements analyzed and varied with season, which is likely due to the impact of 14 coal fired plants located along the Ohio River Valley and secondary sulfate conversion.

4.3. Elemental and organic carbon fractions

Elemental and organic carbon fractions of the measured $PM_{2.5}$ serve as markers for diesel and gasoline engine emissions. Temperature-programmed elemental and organic carbons were measured according to the IMPROVE-TOR and the NIOSH5040-TOT methods to compare results for diesel and gasoline vehicular emissions (Chow et al., 1993, 2001). The concentrations of the elemental and organic carbon fractions as well as the EC/OC ratios are presented in Table 2. EC concentrations ranged from 0.3 ± 0.1 $\mu g/m^3$ (Blue Ash) to 1.3 ± 0.8 $\mu g/m^3$ (St. Bernard) and OC concentrations ranged from 1.6 ± 0.8 (Blue Ash) to 4.9 ± 2.9 $\mu g/m^3$ (St. Bernard), as determined with NIOSH-TOT. However, the IMPROVE-TOR method revealed different EC and OC concentration ranges: 0.5 ± 0.3 to 2.1 ± 1.5 $\mu g/m^3$ and 1.2 ± 0.6 to 3.2 ± 1.0 $\mu g/m^3$, respectively. Differences between the two methods are due to greater influence from charring of organic vapors adsorbed within the quartz-fiber filters on TOT compared to TOR (Chow et al., 2004). However, the TC measured by both methods correlated very well ($r^2 = 0.97$), as shown in Fig. 2. The EC/OC ratio varied from 0.1 to 0.3 (NIOSH method) and 0.2 to 0.6 (IMPROVE method). The higher EC/OC ratio observed at St. Bernard and Brighton. The St. Bernard site located near a major industrial area and a school bus depot; it was also within 400 m from interstate highway I-75, whereas the Brighton site located in the downtown area and close to interstate highway I-75. Different EC/OC ratios reflect the degree of impact of traffic sources on the sampling locations. Certain fractions of EC and OC are rich in diesel and gasoline emissions compared to contributions from other sources, which provides signatures for understanding the difference between traffic

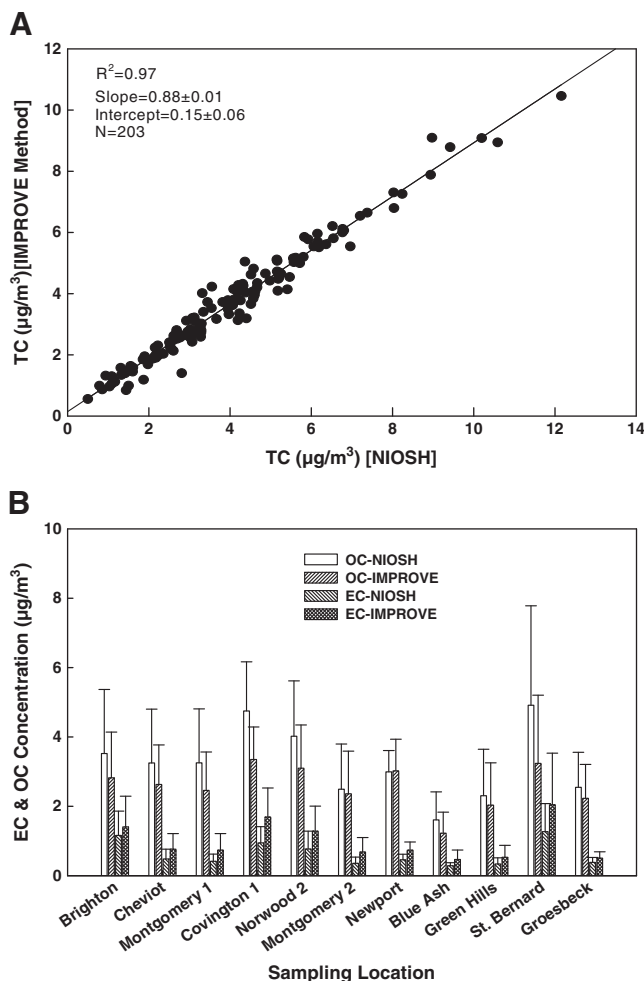


Fig. 2. (A) Correlation between TC estimated from NIOSH method and IMPROVE methodologies. (B) EC and OC variation at different sampling locations estimated from NIOSH and IMPROVE methods.

sources (Cao et al., 2006; Watson et al., 1994). This difference is discussed in Section 4.4.3 in association with the modeling results.

4.4. Results from UNMIX and PMF Modeling

4.4.1. Identified source profiles

Four factors were derived by UNMIX using both EC and OC fractions obtained with the NIOSH method and IMPROVE temperature-resolved eight carbon fractions. The major source factors derived from UNMIX,

Table 2
Elemental and organic carbon concentrations of samples collected at different sites.

Sampling site	NIOSH method ^a			IMPROVE method ^b		
	EC ($\mu g/m^3$)	OC ($\mu g/m^3$)	EC/OC	EC ($\mu g/m^3$)	OC ($\mu g/m^3$)	EC/OC
Brighton	1.2 ± 0.7	3.5 ± 1.9	0.33	1.4 ± 0.9	2.8 ± 1.3	0.50
Cheviot	0.5 ± 0.3	3.3 ± 1.6	0.15	0.8 ± 0.5	2.6 ± 1.1	0.29
Montgomery 1	0.4 ± 0.2	3.3 ± 1.6	0.13	0.7 ± 0.5	2.5 ± 1.1	0.30
Covington1	1.0 ± 0.5	4.8 ± 1.4	0.20	1.7 ± 0.8	3.4 ± 0.9	0.51
Norwood 2	0.8 ± 0.5	4.0 ± 1.6	0.19	1.3 ± 0.7	3.1 ± 1.2	0.41
Montgomery 2	0.4 ± 0.2	2.5 ± 1.3	0.14	0.7 ± 0.4	2.4 ± 1.2	0.29
Newport	0.5 ± 0.2	3.0 ± 0.6	0.15	0.7 ± 0.2	3.0 ± 0.9	0.24
Blue Ash	0.3 ± 0.1	1.6 ± 0.8	0.18	0.5 ± 0.3	1.2 ± 0.6	0.38
Green Hills	0.3 ± 0.2	2.3 ± 1.3	0.15	0.5 ± 0.3	2.0 ± 1.2	0.26
St. Bernard	1.3 ± 0.8	4.9 ± 2.9	0.26	2.1 ± 1.5	3.2 ± 2.0	0.63
Groesbeck	0.4 ± 0.1	2.6 ± 1.0	0.15	0.5 ± 0.2	2.2 ± 1.0	0.23

^a NIOSH-5040 method (Birch and Cary, 1996).

^b IMPROVE temperature protocol (Chow et al., 1993).

based on relative contributions included: combustion related sulfate source (61.9%), traffic source (23.5%), metal processing (11.2%) and soil/crustal source (3.9%). The relative contributions derived from the UNMIX evaluated with eight carbon fractions were similar except for traffic sources (Table 3). PMF identified six sources using two carbon fractions, but could not clearly separate diesel emission source and gasoline vehicle sources. PMF using temperature resolved eight carbon fractions resolved seven sources with clear separation between individual traffic sources. PMF also identified two sulfate sources and one vegetative burning source; whereas these sources were regrouped into one source in UNMIX modeling. The major factors and source estimates derived by PMF are as follows: combustion sulfate (46.8%), vegetative/wood burning (15.8%), metal processing (7.5%), secondary sulfate (12.9%), soil/crustal (0.7%) diesel vehicle emission (10.9%) and gasoline vehicle emission (5.6%). Brief explanations of the derived source profiles by PMF are given below.

4.4.1.1. Sulfate source. PMF identified two sulfate related sources for both the datasets. The percentage contributions estimated by PMF were 46.1% and 10.8% using two carbon fractions, whereas estimated contributions were 46.8% and 12.9% for datasets consisting of eight carbon fractions for combustion sulfate and secondary sulfate, respectively. These sources were characterized by relatively high concentrations of sulfur. The seasonal variation of sulfur concentrations (higher in summer and lower in winter) confirmed that the source is secondary sulfate. These two sources respectively contributed 73.8% and 11.1% to the total sulfur concentrations. Some trace elements Si, Fe, and Al are associated with the secondary sulfate source, which is consistent with previous studies (Liu et al., 2006). The sum of the contributions of both sulfate sources of 56.9% is consistent with the previously reported values of 56% for sulfate related sources (Kim et al., 2004) and in good agreement with the contribution estimated by UNMIX modeling at the CCAAPS sampling site (Hu et al., 2006).

4.4.1.2. Traffic sources. A single traffic source was resolved by applying PMF to a dataset consisting of two carbon fractions. The signatures of this source were a relatively high abundance of EC, OC, Fe, Mn, Cu and Zn fractions. Fe, Cu, Zn are major additives to lubricating oils; Zn is also associated with other transportation activities such as brake and tire wear (Lough et al., 2005) and Mn is an additive are used to improve engine efficiency (Lewis et al., 2003). The estimated EC/OC ratios were 0.35 and 0.81 for two carbon fractions and eight carbon fractions datasets, respectively. The difference in the EC/OC ratios of the derived traffic source profile obtained using two carbon fractions and the temperature resolved eight carbon fractions may be attributed to the different amounts of EC and OC estimated by the two measurement protocols (the NIOSH and IMPROVE methods). This difference is consistent with our ambient analysis, in which the EC fraction estimated by IMPROVE was higher compared to the one determined with the NIOSH method and in most instances OC was lower, although the estimated TC values correlated very well ($R^2 = 0.97$). Lewis et al. (2003) observed the difference in source contribution by applying UNMIX modeling to two carbon fractions analyzed by the NIOSH and

IMPROVE methods, which is consistent with our model results. In a source profile analysis by Watson et al. (1994), the EC/OC ratio was reported to be 0.45 for gasoline-fueled vehicle exhaust, 0.83 for diesel-fueled vehicle exhaust, and 0.90 for a mixture of vehicle types in roadside tests from Phoenix, AZ. Cao et al. (2006) reported EC/OC ratios varying from 0.6 to 1.2 for traffic sources with an average value of 1. In this study, the EC/OC ratios were found to be 0.82 for the traffic source by using temperature resolved eight carbon fractions, which is in close agreement with Cao et al. (2006). The contributions of these two sources were 10.9% and 5.6% respectively for diesel and gasoline vehicle source. The ratio of source contribution estimates of diesel to gasoline vehicle emissions (1.95) is in good agreement with the ratio of 2.3 reported by Kim et al. (2004) at the Jefferson Street monitoring site in Atlanta. Since the E2TC and E3TC fractions present were much lower than E1TC fraction and are mostly below detection limits, the abundances of E1TC were observed in both source profiles.

4.4.1.3. Vegetative/wood burning. Vegetative burning was distinguished by high concentration of OC carbon fractions and high K. Seasonal variation for this source observed as being the highest during winter and low during summer season, confirms that the source is vegetative or wood burning. This factor contributes approximately 15.7% to the total $PM_{2.5}$ and is dominant source of potassium (45.5%).

4.4.1.4. Soil/crustal source. This source factor has high concentrations of Si, Al, Ti, Fe, Ca and K contributing 0.7% to the total $PM_{2.5}$. Crustal particles may include suspended road dust and wind-blown soil dust. The time series source contribution profiles indicated elevated air borne soil/crustal contribution during April and July, 2003 at Cheviot and Bridgeton sampling sites. The elevated soil source contribution during these periods may be caused by wind-blown dust and Asian dust storm. Some carbon fractions were found in this source factor, suggesting some of the airborne soils are re-suspended by road traffic.

4.4.1.5. Metal processing source. Metal processing has abundances of Zn, Pb and Fe and contributes 7.5% of the ambient $PM_{2.5}$ concentration and contains some amount of sulfur in its profiles. The possible reason is that there are several metal processing facilities near the CCAAPS network sampling sites (Hu et al., 2006). This source has also moderate amount of K, which is indicative of the emissions from incinerators.

Source contributions estimated by PMF using two carbon and eight carbon fractions are consistent with the major sources. The comparison of the source profiles derived from the PMF calculation is shown in Fig. 3. The source contribution estimates (Table 3) for metal processing and traffic source by using both the data sets were different. The difference in metal processing source occurred partly because more sources were resolved using eight carbon fractions, thus effectively reducing individual source contributions. The difference in traffic source contribution may be associated with the different analytical technique adopted for EC and OC analysis as described earlier.

4.4.2. Comparison of source profiles derived from UNMIX and PMF

The source profiles identified from UNMIX and PMF using eight carbon fractions are compared in Fig. 4. The larger number of sources

Table 3
Average source contribution (%) to $PM_{2.5}$ estimated from the UNMIX and PMF models (%).

Source	UNMIX with two carbon fractions	UNMIX with eight carbon fractions	PMF with two carbon fractions	PMF with eight carbon fractions
Soil/crustal	3.9 ± 4.1	4.3 ± 4.6	0.6 ± 0.4	0.7 ± 0.4
Vegetative/wood burning			25.3 ± 1.7	15.7 ± 1.0
Combustion sulfate	61.9 ± 8.3	66.4 ± 7.8	46.1 ± 0.6	46.8 ± 0.7
Secondary sulfate			10.8 ± 1.3	12.9 ± 0.5
Metal processing	11.2 ± 3.8	10.17 ± 4.4	7.7 ± 0.4	7.5 ± 0.3
Diesel vehicle				10.9 ± 1.9
Gasoline vehicle				5.6 ± 1.4
Total traffic	23.5 ± 6.2	18.7 ± 5.5	9.5 ± 2.4	16.5

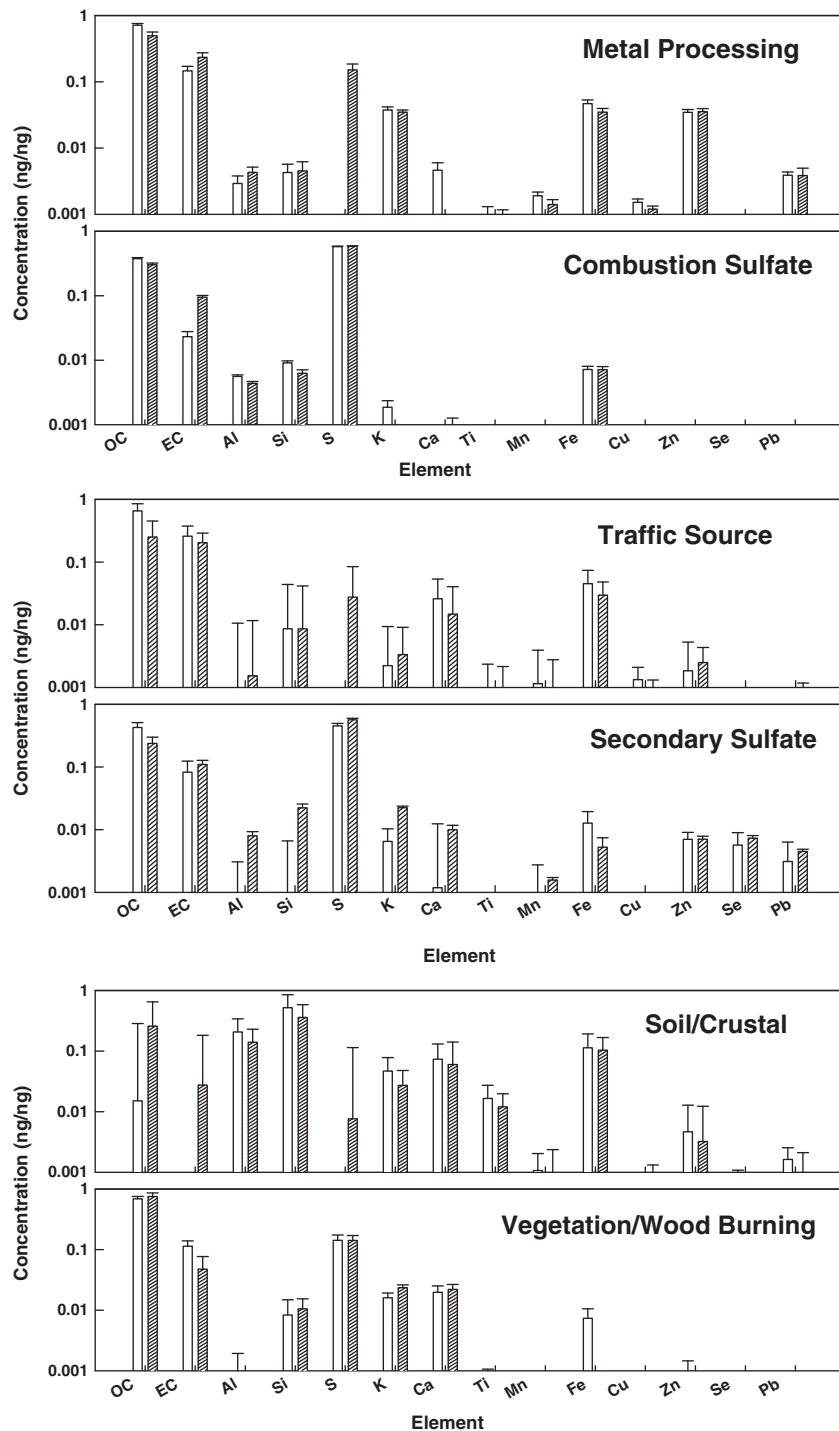


Fig. 3. Comparison of PMF derived source profiles using EC and OC carbon fractions (blank column) and temperature resolved carbon fraction (hatched column).

derived from PMF modeling for the same $PM_{2.5}$ concentrations suggests that PMF predicts lower source estimates than UNMIX for the same sources derived but is able to distinguish more sources. PMF identified two traffic sources, diesel and gasoline vehicular sources, which were combined to form one traffic source for comparison with UNMIX derived traffic source. PMF also identified two additional sources, vegetative burning and secondary sulfate which were not separated in the UNMIX calculation.

The traffic source contribution estimates derived were very close for the eight carbon fractions, 18.7% and 16.5% for UNMIX and PMF,

respectively. PMF derived a secondary sulfate factor, sulfate source and vegetative burning source compared to a single combustion related sulfate source derived by UNMIX. Combined contribution estimates of the two sulfate sources (59.7%) are similar to the one obtained by UNMIX for combustion related sulfate source estimates (66.4%).

The extra source profiles derived from PMF as vegetative burning contribute about 15.7% to $PM_{2.5}$. With seven factors derived from PMF compared to four factors by UNMIX, the crustal elements were distributed in all the sources resulting in lower contribution estimates

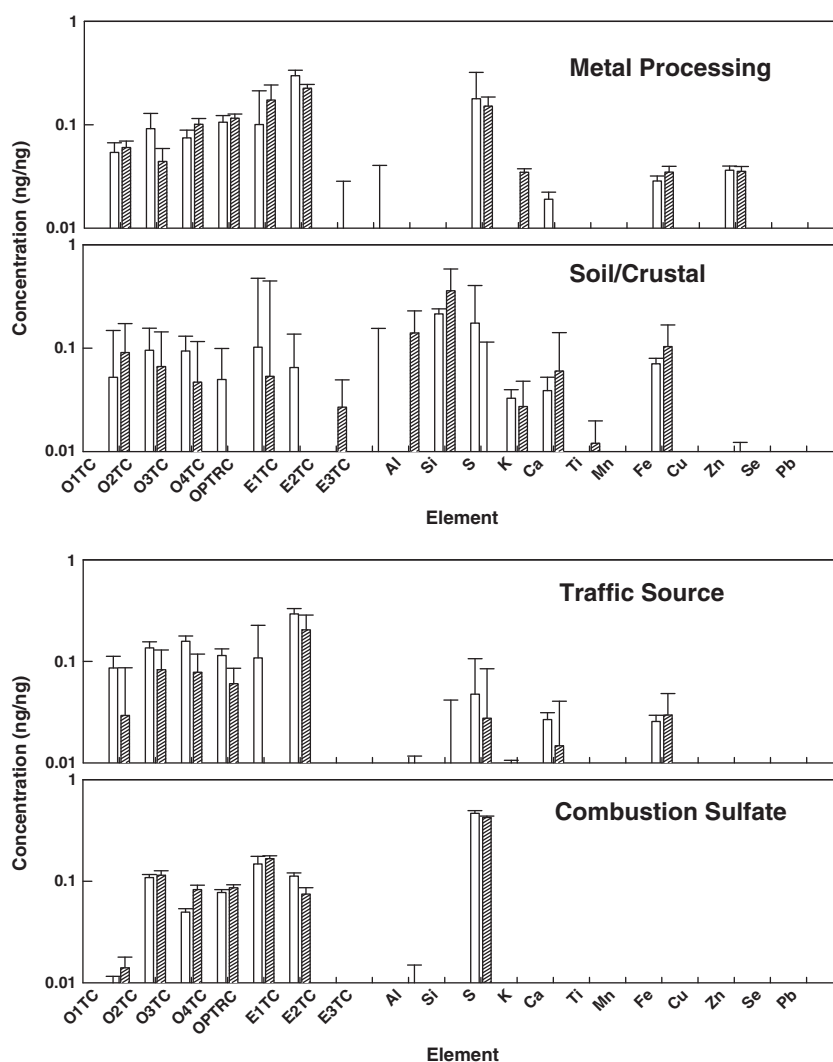


Fig. 4. Comparison of UNMIX (blank) and PMF (hatched bar) source profiles derived from temperature resolved eight carbon fractions (O1TC at 120 °C, O2TC at 250 °C, O3TC at 450 °C, and O4TC at 550 °C in a 100% helium (He) atmosphere). The three EC fractions were measured in a mixture of 2% oxygen/98% He: E1TC at 550 °C, E2TC at 700 °C, and E3TC at 800 °C. Pyrolyzed carbon (OPTRC) is determined based on the laser response (laser reflectance is monitored until it returns to its initial value).

derived by PMF for crustal source. Higher abundances of sulfur were observed in the UNMIX-derived source profiles because all the sulfur were distributed among four factors in UNMIX modeling. The major source profiles derived by both UNMIX and PMF are in good agreement and provide high confidence in the modeling results. Source contribution estimates derived from UNMIX and PMF using both two and eight carbon fractions are presented in Table 3.

4.4.3. Comparison of the traffic source profiles to those referred in literature

The individual EC and OC fractions attributed to gasoline and diesel emissions sources identified in this study were compared (Fig. 5) to the PMF-determined carbon fractions reported in literature for the urban Washington DC (Kim and Hopke, 2004b), Georgia and Alabama (Liu et al., 2006), and a source sampling study performed in Hong Kong (Cao et al., 2006). The diesel vehicle source identified has high concentration of O2TC and E1TC, whereas gasoline source has high concentrations of O3TC and O4TC. This is consistent with the results reported for Washington DC and Jefferson Street in Atlanta (Kim and Hopke, 2004b; Kim et al., 2004). The source sampling study by Watson et al. (1994) found abundant E2TC and O1TC in diesel vehicle exhaust and abundant E1TC in gasoline vehicle exhaust, and Cao et al.

(2006) found a greater abundance of E2TC and O2TC in diesel vehicle exhaust and abundant O3TC and O2TC in gasoline vehicle exhaust. The results qualitatively agree well with the diesel vehicle source estimated at Washington and Atlanta sites. However, large variations in the gasoline vehicle source were observed in all source apportionment studies, which is similar to the observations made by Lee et al. (2006). The relatively high variations may be due to vehicles operating in stop-and-go fashion and the various intersections of interstate highways run with in the CCAAPS sampling network, since intersections create frequent traffic congestion.

4.4.4. Traffic exposure ECAT and ECAD estimation

Traffic sources are the major contributor to EC and OC fractions of PM_{2.5}. The relative contributions estimated from PMF modeling for diesel vehicle emissions source was 10.9% compared to gasoline powered vehicle emissions of 5.6%. The elemental carbons attributed to diesel vehicle source (ECAD) and gasoline vehicle source (ECAG) were separately calculated using the diesel vehicle and gasoline vehicle source derived from PMF. While this calculation is based on limited number of samples that may not accurately represent the EC values, it provides a comparison among different sites and relative impact of traffic sources at these sites. The estimated ECAT and

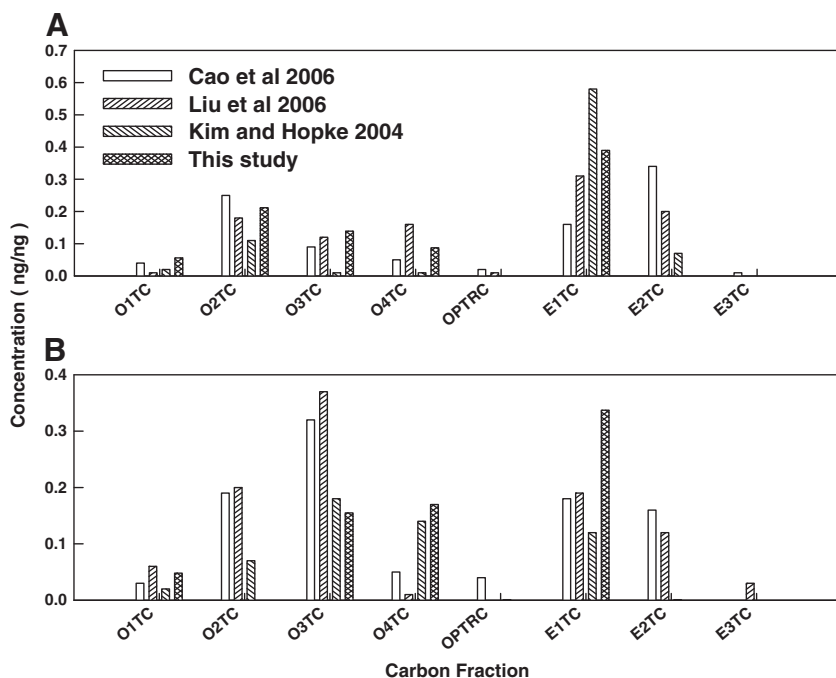


Fig. 5. Comparison of PMF derived traffic source profiles using temperature resolved carbon fractions with literature reported values for carbon sub fractions for: (A) Diesel vehicle emissions, and (B) Gasoline vehicle emissions. (PMF analysis for Greater Cincinnati site (this study), Urban Washington DC (Kim and Hopke, 2004b), Georgia and Alabama site (Liu et al., 2006), and Hong Kong, (Cao et al., 2006)).

ECAD values are listed in Table 4 for various locations. ECAT values were high at sites closer to major truck routes, e.g., at St. Bernard and Bridgton (where I-74 merges with I-75), Covington1 (close to merging point of I-71 and I-75), Newport (very close to I-471) and Norwood2 (400 m from SR-562). Lower ECAT and ECAD values were estimated at relatively clean suburban areas such as Blue Ash as well as Cheviot, Green Hills (suburbs, distant from highways), and Montgomery1 (clean area, further from I-275). This finding confirms the association between ECAT values and relevant traffic sources. ECAT and ECAD values demonstrate that the inner city population is generally exposed to higher levels traffic emissions than the suburban population. Large variations in the ECAT and ECAD estimates were observed at sampling sites located in close proximity to major roads such as Norwood2 (400 m from SR-562), Montgomery 2 (within 400 m from I-71), Blue Ash (close to I-275), Newport (close to I-471) and St. Bernard (close to school bus depot, within 400 m from I-75). The ECAT findings from this study (i.e. combined ECAD and ECAG) are

consistent with our previously reported ECAT values, which were estimated using only two carbon fractions (Ryan et al., 2007). This consistency is also related to generally the small contribution that gasoline, ECAG, makes to the ECAT values. The variations suggest that other factors such as traffic volumes and meteorological parameters are important apart from the proximity of the interstate highways (Hu, 2007). Less variation in ECAT values among suburban sites indicates that they were beyond the impact distance of traffic sources and least affected by variation in traffic pattern. Traffic source emissions and exposures depend also on vehicle operational mode and stop-and-go at specific locations (Shah et al., 2004).

5. Conclusions

The ambient PM_{2.5} samples collected at CCAAPS monitoring sites over five years were analyzed for PM_{2.5} mass, elemental and carbon (EC and OC) concentrations. Two receptor models, UNMIX and PMF, were

Table 4
Elemental carbon concentrations ($\mu\text{g}/\text{m}^3$) attributed to different traffic sources from PMF and UNMIX model calculations: ECAT = Cumulative traffic, ECAG = Gasoline, and ECAD = Diesel.

Location	8 Carbon fractions (PMF)			8-Carbon fractions (UNMIX) ^a	2-Carbon fractions (PMF) ^a	Literature values (Ryan et al., 2007) ^b
	ECAD (Diesel)	ECAG (Gasoline)	ECAT	ECAT	ECAT	ECAT
Bridgton	0.62 ± 0.53	0.12 ± 0.12	0.75 ± 0.63	0.79 ± 0.73	0.47 ± 0.49	0.96
Cheviot	0.19 ± 0.19	0.078 ± 0.08	0.26 ± 0.21	0.29 ± 0.32	0.13 ± 0.17	0.40
Montgomery1	0.22 ± 0.23	0.07 ± 0.07	0.28 ± 0.25	0.45 ± 0.39	0.12 ± 0.14	0.28
Covington1	0.43 ± 0.26	0.21 ± 0.10	0.63 ± 0.31	0.63 ± 0.35	0.44 ± 0.26	0.69
Norwood2	0.54 ± 0.41	0.22 ± 0.21	0.76 ± 0.57	0.77 ± 0.65	0.50 ± 0.47	0.72
Montgomery2	0.35 ± 0.26	0.09 ± 0.05	0.44 ± 0.31	0.47 ± 0.31	0.25 ± 0.22	0.38
Newport	0.54 ± 0.11	0.06 ± 0.04	0.60 ± 0.15	0.80 ± 0.53	0.32 ± 0.12	0.58
Blue ash	0.13 ± 0.12	0.05 ± 0.05	0.18 ± 0.08	0.08 ± 0.11	0.05 ± 0.04	0.45
Green Hills	0.09 ± 0.12	0.07 ± 0.03	0.16 ± 0.12	0.32 ± 0.27	0.06 ± 0.08	0.35
St. Bernard	1.22 ± 1.00	0.45 ± 0.77	1.66 ± 1.71	0.87 ± 0.77	1.09 ± 1.23	1.02
Groesbeck	0.29 ± 0.06	0.05 ± 0.05	0.35 ± 0.05	0.29 ± 0.17	0.16 ± 0.07	0.28

Sites of merging Interstates – St. Bernard and Bridgton, Covington1.

Sites within 400 m of highway – Newport, Norwood2, Montgomery2, Blue Ash, Groesbeck.

Suburban beyond 400 m of highway – Cheviot, Green Hills, Montgomery1.

^a Model results could not differentiate diesel and gasoline vehicle sources.

^b Samples collected from December 2001 to December 2004.

applied to PM_{2.5} data consisting of two carbon fractions measured by NIOSH method and eight carbon fractions determined by IMPROVE method. Based on the source signatures, UNMIX identified only four major sources using both datasets. The source categories identified by UNMIX were combustion related sulfate, metal processing, traffic and soil/crustal. PMF identified six and seven sources by applying two and eight carbon fractions, respectively. Two sulfate sources were resolved, including a sulfate rich source and secondary sulfate source. One vegetation burning source was identified based on the high abundance of OC fractions. The application of PMF allowed to clearly differentiate PM emissions from diesel- and gasoline-powered vehicles using eight carbon fractions. Moreover, PMF could separate the combustion related source from the sulfate rich source which were merged in the UNMIX modeling. This study indicated that using eight carbon fractions can improve source identification and that the PMF model can extract more sources than UNMIX modeling. The difference in the two models, however, is less than one standard deviation. However, we acknowledge the limitation of modeling associated with a limited number of samples. Resolved sources from both models were compared and agreed reasonably well for the major sources identified. ECAT and ECAD values were estimated for different locations and found to vary depending on the proximity of highways as well as factors such as traffic counts, meteorology and operational mode of the vehicles. These markers of traffic-related air pollution will be utilized in land-use regression models to assess childhood exposure to particles arising from the combustion of diesel and gasoline.

Acknowledgments

This work has been supported by the National Institute of Environmental Health and Sciences as a part of the study “Diesel, Allergens and Gene Interaction and Child Atopy” (Grant no. R01 ES11170). Manoranjan Sahu and Pratim Biswas acknowledge partial support from the McDonnell Academy Global Energy and Environmental Partnership (MAGEEP, <http://mageep.wustl.edu>).

Appendix A. Supplementary data

Supplementary data to this article can be found online at doi:[10.1016/j.scitotenv.2011.03.032](https://doi.org/10.1016/j.scitotenv.2011.03.032).

References

- Birch ME, Cary RA. Elemental carbon-based method for monitoring occupational exposures to particulate diesel exhaust. *Aerosol Sci Technol* 1996;25:221–41.
- Cao JJ, Lee SC, Ho KF, Fung K, Chow CJ, Watson JG. Characterization of roadside fine particulate carbon and its eight fractions in Hongkong. *Aerosol Air Qual Res* 2006;6:106–22.
- Chow JC, Watson JG, Pritchett LC, Pierson WR, Frazier CA, Purcell RG. The Dri Thermal optical reflectance carbon analysis system — description, evaluation and applications in United States air-quality studies. *Atmos Environ Part A* 1993;27:1185–201.
- Chow JC, Watson JG, Crow D, Lowenthal DH, Merrifield T. Comparison of IMPROVE and NIOSH carbon measurements. *Aerosol Sci Technol* 2001;34:23–34.
- Chow JC, Watson JG, Chen LWA, Arnott WP, Moosmuller H. Equivalence of elemental carbon by thermal/optical reflectance and transmittance with different temperature protocols. *Environ Sci Technol* 2004;38:4414–22.
- Chow JC, Watson JG, Chen LWA, Chang MCO, Robinson NF, Trimble D, et al. The IMPROVE-A temperature protocol for thermal/optical carbon analysis: maintaining consistency with a long-term database. *J Air Waste Manage Assoc* 2007;57:1014–23.
- EPA US. Health Assessment Document for Diesel Engine Exhaust, Prepared by the National Center for Environmental Assessment Washington DC, for the Office of Transportation and Air Quality. EPA/600/8-90/057F. Available:<http://cfpub.epa.gov/ncea/cfm/recordisplay.cfm?deid=29060>. 2002 Washington D.C.
- Gehrig R, Buchmann B. Characterising seasonal variations and spatial distribution of ambient PM₁₀ and PM_{2.5} concentrations based on long-term Swiss monitoring data. *Atmos Environ* 2003;37:2571–80.
- Henry RC. Multivariate receptor modeling by N-dimensional edge detection. *Chemom Intell Lab Syst* 2003;65:179–89.
- Hetland RB, Refsnes M, Cassee FR, Lag M, Dybing E, Schwarze PE. Cytokine release from alveolar macrophages exposed to ambient particulate matter: relation to size, city, season and metal content. *Toxicol Lett* 2005;158:S80–1.
- Hu S. Approaches to estimating exposure levels of diesel exhaust particles (DEP) in an urban airshed: Model development and applications. Department of Energy, Environmental and Chemical engineering. PhD Washington University in Saint Louis, Saint Louis, 2007.
- Hu SH, McDonald R, Martuzevicius D, Biswas P, Grinshpun SA, Kelley A, et al. UNMIX modeling of ambient PM_{2.5} near an interstate highway in Cincinnati, OH, USA. *Atmos Environ* 2006;40:S378–95.
- Jerrett M, Shankardas K, Berhane K, Gauderman WJ, Kunzli N, Avol E, et al. Traffic-related air pollution and asthma onset in children: a prospective cohort study with individual exposure measurement. *Environ Health Perspect* 2008;116:1433–8.
- Kim E, Hopke PK. Improving source identification of fine particles in a rural northeastern US area utilizing temperature-resolved carbon fractions. *J Geophys Res Atmos* 2004a;109:D09204.
- Kim E, Hopke PK. Source apportionment of fine particles in Washington, DC, utilizing temperature-resolved carbon fractions. *J Air Waste Manage Assoc* 2004b;54:773–85.
- Kim E, Hopke PK, Edgerton ES. Improving source identification of Atlanta aerosol using temperature resolved carbon fractions in positive matrix factorization. *Atmos Environ* 2004;38:3349–62.
- Kim E, Hopke PK, Qin YJ. Estimation of organic carbon blank values and error structures of the speciation trends network data for source apportionment. *J Air Waste Manage Assoc* 2005;55:1190–9.
- Kreyling WG, Semmler M, Erbe F, Mayer P, Takenaka S, Schulz H, et al. Translocation of ultrafine insoluble iridium particles from lung epithelium to extrapulmonary organs is size dependent but very low. *J Toxicol Environ Health A* 2002;65:1513–30.
- Lee JH, Hopke PK, Turner JR. Source identification of airborne PM_{2.5} at the St. Louis-Midwest Supersite. *J Geophys Res Atmos* 2006;111 D10s10.
- Lewis CW, Norris GA, Conner TL, Henry RC. Source apportionment of phoenix PM_{2.5} aerosol with the Unmix receptor model. *J Air Waste Manage Assoc* 2003;53:325–38.
- Liu W, Wang YH, Russell A, Edgerton ES. Enhanced source identification of southeast aerosols using temperature-resolved carbon fractions and gas phase components. *Atmos Environ* 2006;40:S445–66.
- Lough GC, Schauer JJ, Park JS, Shafer MM, Deminter JT, Weinstein JP. Emissions of metals associated with motor vehicle roadways. *Environ Sci Technol* 2005;39:826–36.
- Martuzevicius D, Grinshpun SA, Reponen T, Gorny RL, Shukla R, Lockey J, et al. Spatial and temporal variations of PM_{2.5} concentration and composition throughout an urban area with high freeway density — the Greater Cincinnati study. *Atmos Environ* 2004;38:1091–105.
- Maykut NN, Lewtas J, Kim E, Larson TV. Source apportionment of PM_{2.5} at an urban IMPROVE site in Seattle, Washington. *Environ Sci Technol* 2003;37:5135–42.
- Paatero P. Least squares formulation of robust non-negative factor analysis. *Chemom Intell Lab Syst* 1997;37:23–35.
- Pandya RJ, Solomon G, Kinner A, Balmes JR. Diesel exhaust and asthma: hypotheses and molecular mechanisms of action. *Environ Health Perspect* 2002;110:103–12.
- Polissar AV, Hopke PK, Poirot RL. Atmospheric aerosol over Vermont: chemical composition and sources. *Environ Sci Technol* 2001;35:4604–21.
- Reponen T, Grinshpun SA, Trakumas S, Martuzevicius D, Wang Z, LeMasters G, et al. Concentration gradient patterns of aerosol particles near interstate highways in the Greater Cincinnati airshed. *J Environ Monit* 2003;5:557–62.
- Riedl M, Diaz-Sanchez D. Biology of diesel exhaust effects on respiratory function. *J Allergy Clin Immunol* 2005;115:221–8.
- Ryan PH, LeMasters GK, Biswas P, Levin L, Hu SH, Lindsey M, et al. A comparison of proximity and land use regression traffic exposure models and wheezing in infants. *Environ Health Perspect* 2007;115:278–84.
- Ryan PH, LeMasters GK, Levin L, Burkle J, Biswas P, Hu SH, et al. A land-use regression model for estimating microenvironmental diesel exposure given multiple addresses from birth through childhood. *Sci Total Environ* 2008;404:139–47.
- Ryan PH, Bernstein DI, Lockey J, Reponen T, Levin L, Grinshpun S, et al. Exposure to traffic-related particles and endotoxin during infancy is associated with wheezing at age 3 years. *Am J Respir Crit Care Med* 2009;180:1068–75.
- Schildcrout JS, Sheppard L, Lumley T, Slaughter JC, Koenig JQ, Shapiro GG. Ambient air pollution and asthma exacerbations in children: an eight-city analysis. *Am J Epidemiol* 2006;164:505–17.
- Seagrave J, McDonald JD, Gigliotti AP, Nikula KJ, Seilkop SK, Gurevich M, et al. Mutagenicity and in vivo toxicity of combined particulate and semivolatile organic fractions of gasoline and diesel engine emissions. *Toxicol Sci* 2002;70:212–26.
- Shah SD, Cocker DR, Miller JW, Norbeck JM. Emission rates of particulate matter and elemental and organic carbon from in-use diesel engines. *Environ Sci Technol* 2004;38:2544–50.
- Shi JP, Harrison RM, Brear F. Particle size distribution from a modern heavy duty diesel engine. *Sci Total Environ* 1999;235:305–17.
- Sucharew H, Ryan PH, Bernstein DI, Succop P, Hershey GKK, Lockey JE, et al. Exposure to traffic exhaust and night cough during early childhood: the CCAAPS cohort. *Pediatr Allergy Immunol* 2010;21:253–9.
- Sun QH, Wang AX, Jin XM, Natanzon A, Duquaine D, Brook RD, et al. Long-term air pollution exposure and acceleration of atherosclerosis and vascular inflammation in an animal model. *J Am Med Assoc* 2005;294:3003–10.
- Trenga CA, Sullivan JH, Schildcrout JS, Shepherd KP, Shapiro GG, Liu LJS, et al. Effect of particulate air, pollution on lung function in adult and pediatric subjects in a Seattle panel study. *Chest* 2006;129:1614–22.
- Watson JG, Chow JC, Lowenthal DH, Pritchett LC, Frazier CA, Neuroth GR, et al. Differences in the carbon composition of source profiles for diesel-powered and gasoline-powered vehicles. *Atmos Environ* 1994;28:2493–505.
- Watson JG, Chen LWA, Chow JC, Doraiswamy P, Lowenthal DH. Source apportionment: findings from the US supersites program. *J Air Waste Manage Assoc* 2008;58:265–88.
- Wichmann HE. Diesel exhaust particles. *Inhalation Toxicol* 2007;19:241–4.